Superstability of Surface Nanobubbles

Bram M. Borkent,[1,2] Stephan M. Dammer,[1,2] Holger Schönherr,[2,3] G. Julius Vancso,[2,3] and Detlef Lohse[1,2]

[1]*Physics of Fluids, Faculty of Science and Technology and J. M. Burgers Centre for Fluid Dynamics, University of Twente, P.O. Box 217, 7500 AE Enschede, The Netherlands*

[2]MESA$^+$ *Institute for Nanotechnology, University of Twente, P.O. Box 217, 7500 AE Enschede, The Netherlands*

[3]*Materials Science and Technology of Polymers, Faculty of Science and Technology, University of Twente, P.O. Box 217, 7500 AE Enschede, The Netherlands*

(Received 13 January 2007; published 16 May 2007)

Shock wave induced cavitation experiments and atomic force microscopy measurements of flat polyamide and hydrophobized silicon surfaces immersed in water are performed. It is shown that surface nanobubbles, present on these surfaces, do *not* act as nucleation sites for cavitation bubbles, in contrast to the expectation. This implies that surface nanobubbles are not just stable under ambient conditions but also under enormous reduction of the liquid pressure down to -6 MPa. We denote this feature as *superstability*.

DOI: 10.1103/PhysRevLett.98.204502 PACS numbers: 47.55.dp, 68.08.−p, 68.37.Ps

In recent years, numerous experiments revealed the existence of nanoscopic soft domains at the liquid-solid interface, see [1–10] and references therein. Most experiments employ atomic force microscopy (AFM) [1–8], but other techniques [9,10] have been used as well. The most consistent interpretation of these experiments is that the soft domains, which resemble spherical caps with heights of the order of 10 nm and diameters of the order of 100 nm, are so-called *surface nanobubbles*, i.e., nanoscale gas bubbles located at the liquid-solid interface. This claim is, for instance, supported by the fact that nanobubbles can be merged by the tip of an AFM to form a larger bubble [2], or by the fact that they disappear upon degassing of the liquid [6,7,9], or by the gas concentration dependence of their density [8].

Surface nanobubbles are puzzling objects. First, *they should not exist*: according to the experimental data these bubbles have a radius of curvature R of the order of 100 nm, and therefore (due to a large Laplace pressure inside of the bubbles) they should dissolve on time scales far below a second [11,12]. In marked contrast the experiments show that nanobubbles are stable for hours. Second, they are potential candidates to explain various phenomena associated with the liquid-solid interface, such as liquid slippage at walls [13–15] or the anomalous attraction of hydrophobic surfaces [1] in water. In addition, heterogeneous cavitation usually starts from gaseous nuclei at solid surfaces (see [16] and references therein), and surface nanobubbles are suggested as potential inception sites [7,17,18]. However, apart from convincing experimental evidence for the existence and stability of nanobubbles, still little is known. For instance, why are they apparently stable or how do they react to environmental changes?

In this Letter it is shown that surface nanobubbles, contrary to the expectation, do *not* act as nucleation sites for shock wave induced cavitation on surfaces, where a large tensile stress is created in the water. Hence, yet another puzzle is added to the nanobubble paradox: They are not only stable under ambient conditions but also under enormous reduction of the water pressure down to -6 MPa. We denote this phenomenon as *superstability*.

To demonstrate the superstability of nanobubbles we combine cavitation experiments and AFM measurements. More precisely, cavitation experiments (similar to [18–20]) with different hydrophobic substrates submerged in water are performed: a shock wave generates a large tensile stress (≈ -6 MPa) in the water which leads to cavitation of bubbles at the substrates. The size of the cavitation bubbles is of the order of several hundred μm. Thus, though the bubbles originate from smaller nuclei, they can be visualized by optical means. In addition, AFM measurements of the same substrates in water at ambient conditions are performed to proof and quantify the existence of stable nanobubbles on these substrates. Combining the cavitation and AFM experiments allows to study the relation between cavitation activity and nanobubbles. An analogous strategy has been used previously [20] to perfectly correlate the appearance of surface bubbles in cavitation experiments to the existence of gas-filled microcavities (i.e., microbubbles) of diameter of 2–4 μm which had been etched into the surface. Is there a similar connection between cavitation on smooth unstructured surfaces and surface nanobubbles?

In other words: to what extent must the liquid pressure p_L be reduced to grow a nanoscale bubble to a visible size (i.e., above microns)? A first estimate is obtained from the criterion that unstable growth of a bubble occurs when p_L falls below the critical pressure $p_L^c = p_0 - p_B$, with the ambient static pressure p_0 and the Blake threshold p_B [21,22]. The hemispherical dynamics of a surface bubble under rapid decrease of the liquid pressure is close to that of a free bubble with the same radius of curvature [19].

Therefore, though surface nanobubbles are spherical caps rather than free spherical bubbles, one may obtain a reasonable estimate by the assumption of a spherical bubble. Assuming a nanoscale bubble with radius $R = 100$ nm and $p_0 = 1$ atm one arrives at $p_L^c \approx -0.55$ MPa which is exceeded in the experiments by more than an order of magnitude; see Fig. 1. Moreover, we solved the Rayleigh-Plesset equation [21,22] (which describes the dynamics of a spherical bubble under variations of the liquid pressure) numerically for a gas bubble with the measured liquid pressure reduction as driving force. This calculation yields that bubbles down to a radius of curvature $R = 10$ nm should grow to visible bubbles during the experiments. Hence, theoretically it should be no problem to nucleate a surface nanobubble to visible size, but is this reflected in the experiments?

The setup for the cavitation experiments is similar to that used in [18–20]. A shock wave generator generates a pressure signal in the water, consisting of a high pressure front followed by a large tensile stress; see Fig. 1. The substrate of interest is processed and handled inside a filtered flow bench and placed inside of a sterile flask filled with pure water (Milli-Q Synthesis A10, Millipore), ensuring clean-room conditions throughout the experiment. The flask is placed inside the water tank such that the shock wave is focused onto the substrate. The pressure signal at this position is recorded with a fiber optic probe hydrophone. The cavitation event is photographed by a CCD camera through a long-distance microscope. The major difference between the present setup and that of [18–20] is the maintenance of clean-room conditions by use of the protective flask. Compared to Fig. 2 of Ref. [18] less than 1% cavitation activity on the surface is observed when clean-room conditions are preserved, indicating that contaminations play a dominant role for cavitation experiments under ambient lab conditions.

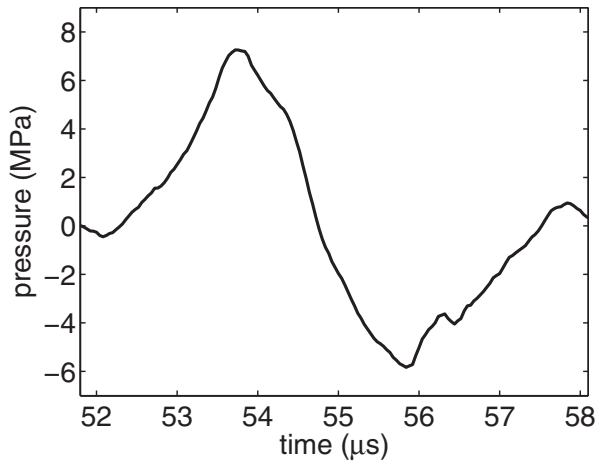

FIG. 1. Pressure signal from the shock wave generator recorded inside of the protective flask with the fiber optic probe hydrophone close to the surface of the chip. The line depicts the low pass filtered signal averaged over five recordings. Triggering the shock wave generator corresponds to time $t = 0$.

The AFM data are acquired on a VEECO/Digital Instruments (DI) multimode AFM equipped with a NanoScope IIIa controller (DI, Santa Barbara, CA) in tapping mode in water using a DI liquid cell and V-shaped Si_3N_4 cantilevers (Nanoprobes, DI). The data shown for case (D) are obtained after mounting the sample into the AFM while keeping the sample surface covered by water at all times, as described previously [23].

Corresponding to different kinds of substrates and/or different procedures of substrate preparation, we present results associated with four different kinds of probes, labeled (A)–(D). Probes (A) and (B) use smooth polyamide surfaces as solid substrate. Polyamide is heated and molded between silicon and atomically smooth mica. The mica is removed when the polyamide is cooled down to room temperature, leaving a relatively smooth polyamide surface with a root mean square (rms) roughness of 3.5 nm (measured by AFM on 1×1 μm^2) and a static contact angle of 80°. Besides large smooth areas of many mm^2 the production process also creates several microscopic cracks in the surface. In case (A) these polyamide surfaces are used in the experiments without further treatment. In case (B) the substrate is first covered by ethanol which is then flushed away by water. This ethanol-water exchange has been reported to induce the formation of surface nanobubbles; see [5,8] and references therein. Besides the explanation suggested in [5] we note that also the exothermic mixing [24] of ethanol and water might induce the formation of nanobubbles, since a temperature increase favors the formation of nanobubbles [8]. In the cavitation experiments a drop of ethanol is placed on the substrate such that it is completely covered by ethanol before it is submerged in water. Then the substrate is moved inside the protective flask for a minute to replace the miscible ethanol by water [25]. In the AFM experiment for case (B) a liquid cell is used.

Probes (C) and (D) use pieces of smooth hydrophobized silicon as the substrate. A Si(100) wafer is diced into chips (1×1 cm^2) which are immersed for 15 minutes in a (5:1) Piranha cleaning mixture. Hereafter, the chips are hydrophobized by chemical vapor deposition of 1H,1H,2H,2H-perfluorodecyldimethylchlorosilane (PFDCS) [18], yielding a rms value of ≈ 0.36 nm (measured by AFM on 1×1 μm^2), a coating thickness ≈ 2.6 nm (measured by ellipsometry), and an advancing contact angle $\approx 100°$. Note that the silane film is not able to move; it is a stable self-assembled monolayer covalently bonded to the underlying substrate. Before immersion in water the probes are rinsed with ethanol and blown dry with argon gas [18]. Case (D) additionally applies the *ex situ* ethanol-water exchange as described above.

In each of the cases (A)–(C) substrates of the respective type are produced in an identical manner. One substrate is used in the cavitation experiments and one in the AFM measurements. Note that we checked that the observed cavitation activity and nanobubble density were reproducible among substrates of the same kind. Furthermore, in

case (D) the *same* substrate is used in both experiments. After the cavitation experiment (exposure to a single shock wave) the substrate is transported in water to the AFM, where it is mounted without exposure to air, whereafter the water-solid interface is imaged as it appears after the cavitation experiments.

Do substrates with a high nanobubble density show a large cavitation activity? Figure 2 illustrates the experimental results. The left panel shows typical recordings of the cavitation experiments for the cases (A)–(D). The right panel shows the corresponding AFM-measurements of the substrate surfaces immersed in water. Though the substrates have relatively large contact angles and the water pressure drops down to ≈ -6 MPa during the experiments there is hardly any cavitation on the smooth substrates (A)–(D). Note that the cavitation bubbles in (A) originate exclusively from microscopic cracks in the surface, as can be seen in Fig. 2(A). Applying the ethanol-water exchange, these microcracks do not lead to surface cavitation; see Fig. 2(B). Contrary to the cavitation experiments, the AFM measurements show that all substrates are densely covered by surface nanobubbles, with number densities between 10

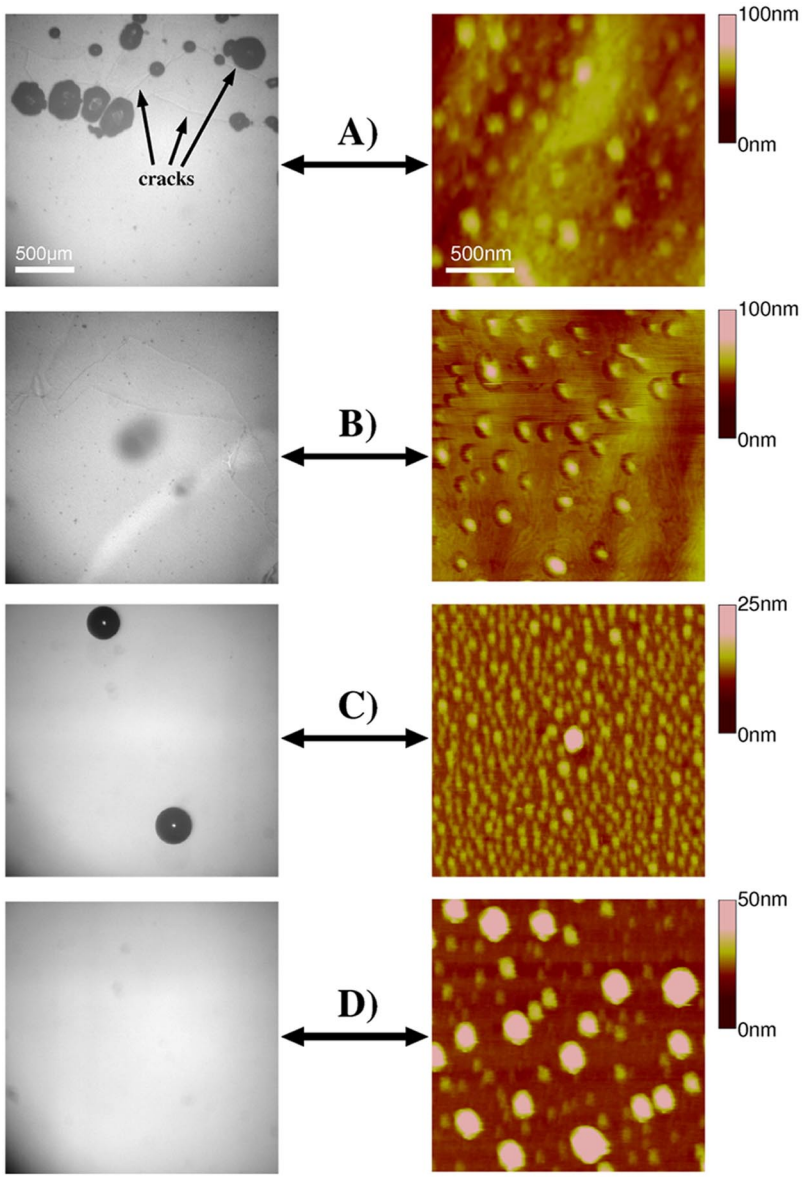

FIG. 2 (color online). Cavitation activity (left), and corresponding nanobubble density (right) imaged by AFM (topography images) for various probes. The length scales given in (A) also refer to (B), (C), and (D). (A) and (B): polyamide substrates; (B) after ethanol-water exchange (see text). (C) and (D): hydrophobized silicon substrates; (D) after ethanol-water exchange. Scanning velocities for the cases (A)–(D) are 46, 20, 10, and 40 μm/s, respectively. There is hardly any cavitation though the substrates are densely covered by surface nanobubbles. Note that the cavitation bubbles in (A) emerge exclusively from microscopic cracks in the surface, whereas the whole substrate is covered by nanobubbles. The cavitation bubbles in (C) presumably originate from surface contaminations. In (D) it is shown that nanobubbles are still stably present *after* the cavitation experiments.

and 80 bubbles per μm^2. The sizes range from 3 to 40 nm in height and 60 to 300 nm in diameter. Several standard tests were performed (not shown) to ensure that the structures seen in the AFM images are indeed surface nanobubbles. Force-volume measurements [1,3,5] and tip manipulation of the bubbles [2] are in accordance with previous studies. Furthermore, nanobubbles are not present when the substrates are immersed in ethanol, in agreement with [8]. Successive cycles of ethanol-water and water-ethanol exchange resulted in pictures without (in ethanol) and with nanobubbles (in water). Finally, when degassed ethanol is exchanged by degassed water, nanobubbles are *not* induced.

Thus the combination of the cavitation and the AFM experiments yields the remarkable result that the surface nanobubbles do not cavitate, in spite of the enormous tensile stress they are exposed to. This contradicts the expectation that the experimental pressure signal should be able to cavitate bubbles with an initial radius of curvature down to 8 nm. Case (D) explicitly shows that nanobubbles are still present *after* [26] the cavitation experiments, and that there is no cavitation activity at the surface induced by the shock wave. While it is already puzzling that surface nanobubbles are stable under ambient conditions, it is even more puzzling that they still exist after the passage of a shock wave with a large tensile stress down to ≈ -6 MPa. We denote this as *superstability.*

One may wonder what actually is happening with the surface nanobubbles when the shock wave is passing by. With the present technology it is impossible to AFM image the nanobubbles (which takes order of minutes) during the shock wave passage (which is order of μs). Therefore, evidence can only be indirect.

One may also question whether the nanobubbles survive the compression wave (with typical time scale $\tau \approx 1$ μs so that the nanobubbles respond quasistatically). During the compression phase, gas may diffuse into the neighboring liquid around the bubble. With a typical diffusion constant of $D \approx 10^{-9}$ m^2/s we get as typical diffusion length scale $\sqrt{\tau D} \approx 100$ nm. Hence the liquid close to the remaining void (100 nm) will become supersaturated with gas. However, during the negative pressure phase, i.e., during the expansion of the bubble, all this gas will be recollected by the bubble, as has been shown in Ref. [27] (for micrometer bubbles).

In summary, it is demonstrated that in standard shock wave induced cavitation experiments surface nanobubbles do *not* act as nucleation sites. Cavitation bubbles originate from contaminations or from microscopic structures such as microcracks or microcrevices [19,20], rather than from surface nanobubbles which densely populate the immersed substrates. This implies that surface nanobubbles are unexpectedly stable under large tensile stresses.

We thank Szczepan Zapotoczny for his contribution, K. A. Mørch for discussions, and acknowledge financial support from STW (NanoNed Program), DFG (Grant No. DA969/1-1), the MESA$^+$ Institute for Nanotechnology, and CW-NWO (vernieuwingsimpuls program for H. S.).

[1] J. W. G. Tyrrell and P. Attard, Phys. Rev. Lett. **87**, 176104 (2001).
[2] A. C. Simonsen, P. L. Hansen, and B. Klösgen, J. Colloid Interface Sci. **273**, 291 (2004).
[3] M. Holmberg *et al.*, Langmuir **19**, 10 510 (2003).
[4] A. Agrawal *et al.*, Nano Lett. **5**, 1751 (2005).
[5] X. H. Zhang, N. Maeda, and V. S. J. Craig, Langmuir **22**, 5025 (2006).
[6] L. Zhang *et al.*, Langmuir **22**, 8109 (2006).
[7] X. H. Zhang *et al.*, Langmuir **22**, 9238 (2006).
[8] S. Yang, S. Dammer, S. Kooij, H. Zandvliet, and D. Lohse, Langmuir (to be published).
[9] M. Switkes and J. W. Ruberti, Appl. Phys. Lett. **84**, 4759 (2004).
[10] R. Steitz *et al.*, Langmuir **19**, 2409 (2003).
[11] P. S. Epstein and M. S. Plesset, J. Chem. Phys. **18**, 1505 (1950).
[12] S. Ljunggren and J. C. Eriksson, Colloids Surf. A **129**, 151 (1997).
[13] E. Lauga and M. P. Brenner, Phys. Rev. E **70**, 026311 (2004).
[14] E. Lauga, M. P. Brenner, and H. A. Stone, in *Handbook of Experimental Fluid Dynamics*, edited by C. Tropea, J. Foss, and A. Yarin (Springer, New York, 2005).
[15] C. Neto *et al.*, Rep. Prog. Phys. **68**, 2859 (2005).
[16] A. A. Atchley and A. Prosperetti, J. Acoust. Soc. Am. **86**, 1065 (1989).
[17] M. Holmberg *et al.*, in Cav03-GS-1-001, Fifth International Conference on Cavitation, Osaka, Japan, 2003, http://cav2003.me.es.osaka-u.ac.jp/Cav2003/Papers/Cav03-GS-1-001.pdf.
[18] N. Bremond, M. Arora, C. D. Ohl, and D. Lohse, J. Phys. Condens. Matter **17**, S3603 (2005).
[19] N. Bremond, M. Arora, S. M. Dammer, and D. Lohse, Phys. Fluids **18**, 121505 (2006).
[20] N. Bremond, M. Arora, C. D. Ohl, and D. Lohse, Phys. Rev. Lett. **96**, 224501 (2006).
[21] C. E. Brennen, *Cavitation and Bubble Dynamics* (Oxford University, New York, 1995).
[22] T. G. Leighton, *The Acoustic Bubble* (Cambridge University Press, Cambridge, England, 1994).
[23] K. Morigaki *et al.*, Langmuir **19**, 6994 (2003).
[24] *Rodd's Chemistry of Carbon Compounds*, edited by S. Coffey (Elsevier, Amsterdam, 1965), 2nd ed., Vol. 1, Part. B.
[25] We verified that our *ex situ* ethanol-water exchange generates surface nanobubbles, by placing the processed substrate in the AFM while keeping water on its surface. Then the substrate was AFM scanned and many surface nanobubbles (>10 per μm^2) were observed.
[26] Strictly speaking, we cannot exclude that surface nanobubbles reform prior to the AFM measurements (within minutes), after the cavitation had originally removed them.
[27] S. Hilgenfeldt, D. Lohse, and M. P. Brenner, Phys. Fluids **8**, 2808 (1996).